Modeling of Tension Modulation Nonlinearity in Plucked Strings

Tero Tolonen, *Student Member, IEEE*, Vesa Välimäki, *Senior Member, IEEE*, and Matti Karjalainen, *Member, IEEE*

***Abstract*—In this paper, a nonlinear discrete-time model that simulates a vibrating string exhibiting tension modulation nonlinearity is developed. The tension modulation phenomenon is caused by string elongation during transversal vibration. Fundamental frequency variation and coupling of harmonic modes are among the perceptually most important effects of this nonlinearity. The proposed model extends the linear bidirectional digital waveguide model of a string. It is also formulated as a computationally more efficient single-delay-loop structure. A method of reducing the computational load of the string elongation approximation is described, and a technique of obtaining the tension modulation parameter from recorded plucked string instrument tones is presented. The performance of the model is demonstrated with analysis/synthesis experiments and with examples of synthetic tones available at http://www.acoustics.hut.fi/~ttolonen/tmstr_SAP/.**

***Index Terms*—Acoustic signal processing, modeling, musical acoustics, musical instruments, nonlinear systems, signal synthesis.**

I. Introduction

PHYSICAL modeling is one of the most rapidly advancing areas in computer music and sound synthesis. With multimedia applications emerging into desktop computers and other interactive terminals, physics-based virtual instruments reach a growing consumer group. Algorithms for sound effects and sound synthesis are for the first time being standardized in the proposed MPEG-4 multimedia standard [2]. No doubt, physical modeling is going to play a key role within the area of digital audio in the future.

Physical models are computational algorithms that simulate sound generating mechanisms found, e.g., in musical instruments and the human voice production. From a sound synthesis point of view, the most popular physical modeling approach has been based on the digital waveguide [3]–[5]. In its basic form it is derived from the linear one-dimensional (1-D) wave equation and it is an efficient way to simulate wave propagation in resonators that produce harmonic or nearly harmonic signals, such as a vibrating string or an air column in a wind instrument. Nonlinear extensions to the linear digital waveguide have been presented for the simulation of nonlinear propagation of waves in a trombone [6], [7] and for a string that is terminated with a nonlinear double-spring apparatus [8]. These two cases may be generalized to signal-dependent nonlinearities that can be implemented using a *time-varying fractional delay* (TVFD) filter [9]. Other nonlinear string instrument models include the slap-bass model of Rank and Kubin [10] and the nonlinear commuted synthesis model for the violin by Smith [11]. A model with a memoryless nonlinearity for the kantele, a traditional Finnish plucked string instrument, is presented in [12].

The linear digital waveguide has been extensively used for simulation of wave propagation in a string in synthesis of plucked and struck string instrument sounds; see, e.g., [5] and [13] for references. However, the vibrating string is linear only to the first approximation and, consequently, nonlinear phenomena exhibited by every real string are inherently omitted in the simulation. Perceptually, among the most relevant nonlinear phenomena of a vibrating string are *pitch variation* and variation of timbre due to *nonlinear coupling of the harmonic components*. They are related to the modulation of string tension that is caused by elongation of the string during vibration. Other effects caused by tension modulation include missing overtone generation and partial intermodulation.

Nonlinear vibration of an elastic string has been examined both analytically and experimentally. In 1945, Carrier studied the free undamped motion of a string [14]. His work considered planar transversal wave motion and discarded longitudinal vibrations. In 1967, Narasimha extended Carrier's results and took into account the longitudinal vibrations [15]. It was shown that the two transversal and the longitudinal polarizations are nonlinearly coupled (see also [16]). At the same time Anand [17] showed that the equations of transversal and longitudinal waves are separable if the order of modes of the transverse vibration is small compared to $\sqrt{ES/F_{\mathrm{nom}}}$, where E is Young's modulus, S is the cross-sectional area of the string, and F_{nom} is the nominal string tension. He further showed that under sinusoidal initial conditions the two transversal polarization components possess an oscillatory character. The interaction of transversal and longitudinal wave motion was also tackled in [18]. More recently, experimental results of nonlinear string vibration have been reported. Legge and Fletcher described the coupling of vibrating modes in a one-polarization wave motion and demonstrated the generation of missing harmonics as a result of this coupling [19]. Hansen *et al.* experimented with coupling of polarizations and reported measured results of amplitudes and phase differences of transversal components under forced motion [20]. More interestingly, they found nonlinear coupling of the two transversal polarizations even at vibration displacements of only a few microns.

Manuscript received October 20, 1998; revised June 22, 1999. This work was supported by the GETA Graduate School, Helsinki University of Technology, Jenny ja Antti Wihurin rahasto (the Foundation of Jenny and Antti Wihuri), and the Academy of Finland. Preliminary results of this study were reported in [1]. The associate editor coordinating the review of this manuscript and approving it for publication was Dr.-Ing. Juergen H. Herre.

The authors are with the Laboratory of Acoustics and Audio Signal Processing, Helsinki University of Technology, Espoo FIN-02015, Finland (e-mail: tero.tolonen@hut.fi; http://www.acoustics.hut.fi/~ttolonen).

Publisher Item Identifier S 1063-6676(00)03907-9.

In this paper, we develop a nonlinear discrete-time model that simulates the nonlinearity caused by tension modulation in a string. Our model extends the bidirectional linear digital waveguide model of a string, and we also formulate the model as a computationally efficient *single-delay-loop* structure. The parameters of the model are estimated from recordings of string instrument tones. Audio examples available via the WWW [21] demonstrate that the synthesized tones are more realistic than those produced with a linear model.

The main guideline applied in developing the nonlinear model is perceptual relevance. Our model is not able to accurately simulate all the nonlinear phenomena exhibited by a vibrating string, but it essentially captures the effects that tension modulation nonlinearity has on the tone character. In particular, the proposed model allows parametric control of pitch variation and coupling between the harmonics.

The paper is organized as follows. The vibration of an elastic string exhibiting tension modulation is described in Section II. In Section III, a digital waveguide is formulated for waves with uniformly distributed time-varying propagation speed. Using the results of Section III, the digital waveguide model of a string with tension modulation is described in Section IV. A method for model parameter estimation based on recordings of string instrument tones is described in Section V, and results of synthesis experiments are reported in Section VI. Conclusions are drawn in Section VII.

II. Nonlinearly Vibrating String

In this study, we are interested in autonomous motion of a simply terminated string that vibrates transversally in a plane. We also assume that the propagation speed of the longitudinal vibration is considerably higher than that of the transversal vibration, as is typically the case with strings of musical instruments, so that tension is approximately uniform along the string. In steel strings, for instance, the speed of the longitudinal vibration is approximately 5100 m/s, whereas the speed of transversal vibration in the high-E string (330 Hz, length 0.65 m) is 446 m/s. The string is taken to be linearly elastic, and the inharmonicity caused by string stiffness (dispersion) is assumed negligible. We further assume that the cross-sectional area of the string, and hence its density, is constant during the vibration.

It is clear that these assumptions prohibit accurate simulation of some of the nonlinear phenomena exhibited by a vibrating string, including couplings between the longitudinal and the two transversal polarizations. However, as demonstrated below, the model derived using these assumptions is capable of qualitatively imitating the essential behavior of a string with tension modulation in both functional and perceptual senses. Elaboration of this model to include the three vibrational polarizations remains an interesting future challenge.

The main cause of nonlinearity in a vibrating string is tension modulation that is related to elongation of the string during vibration. Elongation may be expressed as the deviation from the nominal string length $\ell_{\rm nom}$ [19]

$$\ell_{\rm dev} = \int_0^{\ell_{\rm nom}} \sqrt{1+\left(\frac{\partial y}{\partial x}\right)^2}\,dx - \ell_{\rm nom} \tag{1}$$

where y is the displacement of the string and x is the spatial coordinate along the string. It is obvious from (1) that the elongation $\ell_{\rm dev} = 0$ every time the string is in its equilibrium position, and that it oscillates with a period equal to half the period of string vibration.

Tension F_t along the string is linearly related to the elongation $\ell_{\rm dev}$ and it can be expressed as [19]

$$F_t = F_{\rm nom} + \frac{ES\ell_{\rm dev}}{\ell_{\rm nom}} \tag{2}$$

where

$F_{\rm nom}$	nominal tension corresponding to the string at rest;
E	Young's modulus;
S	cross sectional area of the string.

Equation (2) reveals that the tension also oscillates with half the period of the string vibration, as illustrated in Fig. 1. The figure depicts a simulation of tension in a string that is plucked at its midpoint. In this simulation, we assume that the end supports are rigid and that there is only frequency-independent damping that results in the decay of the tone. The simulation is conducted using a dual-delay-line digital waveguide model with distributed losses. The oscillating curve shows the time-varying tension of the string. The monotonically decaying curve illustrates the averaged tension, and it is obtained with a running average computation over segments with length of one tension oscillation period. The dashed line shows the constant value of $F_{\rm nom}$, i.e., the nominal tension corresponding to the string at rest. Note that when the string is plucked at the midpoint, $F_t = F_{\rm nom}$ twice during one period of string oscillation. This is intuitively clear since the displacement $y(x) = 0$ for all x twice in a period. However, when a lossy string is plucked at any other point, the tension only approaches the nominal tension with time.

In the linear case, the propagation speed of the transversal wave is $c_{\rm nom} = \sqrt{F_{\rm nom}/\rho_{\rm nom}}$, where $\rho_{\rm nom}$ is the linear mass density along the string at rest. When we assume that the longitudinal wave propagation speed is considerably larger than the transversal propagation speed, the linear mass density and the tension are approximately spatially constant and we may write the propagation speed of the transversal wave as

$$\begin{aligned} c &= \sqrt{\frac{F_t}{\rho}} = \sqrt{\left(\frac{\ell_{\rm nom}+\ell_{\rm dev}}{\rho_{\rm nom}\ell_{\rm nom}}\right)\left(F_{\rm nom}+\frac{ES\ell_{\rm dev}}{\ell_{\rm nom}}\right)} \\ &= c_{\rm nom}\sqrt{1+\left(1+\frac{ES}{F_{\rm nom}}\right)\frac{\ell_{\rm dev}}{\ell_{\rm nom}}+\frac{ES}{F_{\rm nom}}\left(\frac{\ell_{\rm dev}}{\ell_{\rm nom}}\right)^2} \end{aligned} \tag{3}$$

where ρ is linear mass density of the vibrating string given by $\rho = \rho_{\rm nom}\ell_{\rm nom}/(\ell_{\rm nom}+\ell_{\rm dev})$.

The time-varying tension modifies the effective frequencies of the harmonics. Note that since the propagation velocity of the wave is time-varying, the spatially orthogonal eigenmodes are not separable to sinusoids with constant frequencies in the time variable. Since we are interested in the variation of the fundamental frequency, it is more natural to think in terms of the effective fundamental frequency of vibration, i.e., a fundamental frequency obtained by analysis of the tone or corresponding to

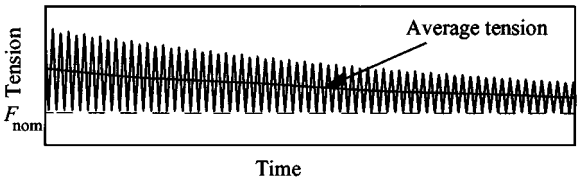

Fig. 1. Tension variation in a simulated vibration of a string is depicted with the oscillating solid line for a string plucked at the midpoint. The average tension is presented with the monotonic decay curve. The dashed line shows the nominal tension that corresponds to the string at rest.

a perceived pitch. In the linear case, the fundamental period of vibration is expressed as

$$T_0 = \lambda / c_{\rm nom} \tag{4}$$

where λ is twice the distance (in meters) between the string terminations. In the nonlinear case, the wave propagation speed is a function of time and thus using directly (4) we would obtain a fundamental period that oscillates with approximately double the period of the lowest spatial mode. Since this is ambiguous, we use the term effective fundamental period to refer to a short-time average value of λ/c. In that sense, we expect the effective fundamental frequency and also the perceived pitch to behave like the average tension curve of Fig. 1. As an example, Fig. 2 illustrates two fundamental frequency trajectories detected from a recorded electric guitar tone (top) and a steel-stringed acoustic guitar tone (bottom). The time constant of the fundamental frequency drift is related to the time constant of the attenuation of the tone [19].

While the average tension explains the time-varying fundamental frequency of the tone, it is not capable of accounting for the coupling between the harmonic modes. Legge and Fletcher showed that such a coupling may only occur when, in addition to the tension modulation, at least one of the end supports is not completely rigid [19]. In the case of rigid end supports, the harmonic modes are always spatially orthogonal and thus they may not interact with each other. In musical instruments the end supports are never completely rigid and mode coupling always takes place.

The assumption that the longitudinal wave propagation velocity is considerably larger than that of the transversal waves leads to a uniform spatial distribution of the transversal velocity. This essentially means that the tension modulation is immediately spread across the string. From a discrete-time simulation viewpoint, this is important since such a wave propagation can be accurately simulated with a computationally efficient structure [9], as described in Section III.

III. Digital Waveguide with Uniformly Time-Varying Propagation Speed

In a linear 1-D bidirectional digital waveguide, waves $y_r(n)$ and $y_l(n)$ travel to the right and to the left, respectively [3], [4]. The output of the waveguide at a discrete time instant n at position k is obtained as

$$y(n,\, k) = y_r(n-k) + y_l(n+k). \tag{5}$$

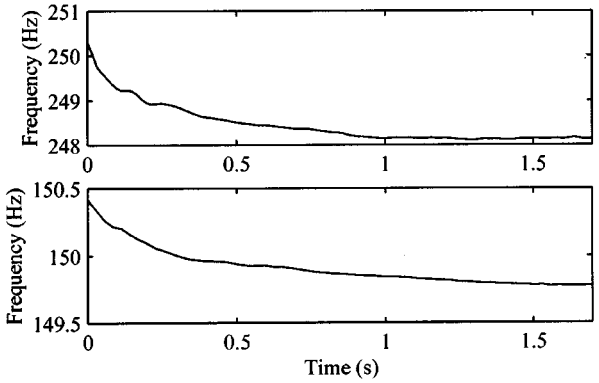

Fig. 2. Time-varying fundamental frequency as detected in (top) a recorded electric guitar tone and (bottom) in a recorded tone of a steel-stringed acoustic guitar.

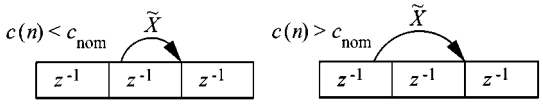

Fig. 3. Wave propagation in a digital waveguide with time-varying velocity for the two cases when the velocity is (left) smaller and (right) larger than the nominal velocity $c_{\rm nom}$.

The wave propagation speed $c_{\rm nom}$ is related to the spatial and temporal sampling intervals X and T as $c_{\rm nom} = X/T$.

When the propagation speed is spatially uniformly distributed and relatively slowly varying in time, the wave travels a distance $\tilde{X} = c(n)T$ between time instances n and $n+1$. Note that $\tilde{X} = X$ only when $c = c_{\rm nom} = X/T$. The time-varying wave propagation is illustrated in Fig. 3 for the two cases where $c(n) < c_0$ and $c(n) > c_0$. Fig. 3 implies that we have to resample the content of the delay lines in each sampling period. While this may be achieved using fractional delay filtering [22], [23], a computationally efficient strategy is required in practice. Furthermore, constant resampling of the traveling wave is bound to degrade the signal since an error is associated with every interpolation operation [23].

A. Efficient Formulation of the Time-Varying Propagation Speed

A more efficient and accurate implementation of the digital waveguide with time-varying uniformly distributed propagation speed can be developed if we only wish to observe the traveling wave at one or a few spatial positions. For reasons of simplicity, we only consider the right-going wave $y(n,\, m) = y_r(n-m)$, in the following; it is straightforward to treat the left-going wave similarly. For convenience in developing the formulation, we assume that the waveguide is lossless. When using the formulation in the actual synthesis model, we will assume that the losses of the string are not significantly altered by the tension modulation so that consolidating the losses into a single linear filter results in a negligible approximation error. Given an initial distribution $y(0,\, m)$, $m = -\infty, \cdots, \infty$, the output at an observation point k at $n = 1$ is given as $y(1,\, k) = y(0,\, k - c(0)T)$, and at $n = 2$

as $y(2,\,k) = y(0,\,k - c(0)T - c(1)T)$, and so on. More generally

$$y(n,\,k) = y\left(0,\,k - T\sum_{l=0}^{n-1} c(l)\right), \qquad n > 0. \tag{6}$$

Note that, as before, we assume that the propagation speed varies relatively slowly in time so that we allow $c(n)$ only to change at sample instants.

We express the time-varying velocity as $c(n) = c_{\rm nom} + c_{\rm dev}(n)$, where $c_{\rm dev}(n)$ is the deviation from the nominal velocity $c_{\rm nom}$, and rewrite (6) as

$$\begin{aligned} y(n,\,k) &= y\left(0,\,k - T\sum_{l=0}^{n-1}[c_{\rm nom} + c_{\rm dev}(l)]\right) \\ &= y\left(0,\,k - nc_{\rm nom}T - T\sum_{l=0}^{n-1} c_{\rm dev}(l)\right). \end{aligned} \tag{7}$$

In (7) the term $nc_{\rm nom}T$ equals a spatial distance nX, i.e., the distance a wave travels with velocity $c_{\rm nom}$ in time n. We can thus compute $y(n,\,k) = y(n-1,\,k-1-T\sum_{l=0}^{n-1} c_{\rm dev}(l))$ if the wave propagates with a constant velocity $c_{\rm nom} = 1/T$ in the digital waveguide. This means the digital waveguide is used as in the linear case with constant velocity, and that the time-varying velocity is taken into account by reading the output with a fractional delay filter. This implies that it suffices to utilize a single fractional delay filter operating in the vicinity of position k and approximating the real-valued delay

$$d(n) = -T\sum_{l=0}^{n-1} c_{\rm dev}(l). \tag{8}$$

Notice that the delay $d(n)$ is the time integral of the speed deviations, and if the mean of $c_{\rm dev}$ is nonzero, the value of parameter $d(n)$ will diverge.

The delay term $d(n)$ depends on the time history of the deviation term $c_{\rm dev}(n)$. This can be interpreted as comprising the locality in time for the locality in position since now we have to store the time history of the deviation term $c_{\rm dev}$ but we only need to apply the fractional delay at a single position in the digital waveguide. When resampling is used, the distance $c(n)T$ depends only on the current velocity value $c(n)$. Note that since we have developed the single-fractional-delay formulation for the waveguide of infinite length, the time history required is infinite in general. However, in practical applications, only the time history of speed deviation that corresponds to the traveling time between two consecutive observation or modification positions in the waveguide is required.

By applying the preceding treatment to the left-going traveling wave, we can generalize the above result for the bidirectional digital waveguide. After a straightforward computation the waveguide output at position k is obtained as

$$\begin{aligned} y(n,\,k) = {} & y_r(n-1,\,k-1+d(n)) \\ & + y_l(n-1,\,k+1-d(n)) \end{aligned} \tag{9}$$

i.e., as a sum of the two traveling waves at position k.

B. Time-Varying Propagation in Digital Waveguide of Finite Length

In practical applications, the waveguides are always of finite length. Let us consider a unidirectional waveguide where two observation points x_1 and x_2 are separated by a delay of $L_{\rm nom}$ samples which is related to a physical distance $\ell_{\rm nom}$ on the string as

$$L_{\rm nom} = \frac{\ell_{\rm nom} f_s}{c_{\rm nom}} \tag{10}$$

where f_s is the sampling rate. Note that the modulation of the delay in the digital waveguide implementation corresponds to modulation of the propagation speed in actual string vibration, i.e., it corresponds to the time it takes the wave to travel the distance $\ell_{\rm nom}$ with varying propagation speed. The delay parameter is in this case obtained as

$$d(n) = -T\sum_{l=n-1-\hat{L}_{\rm nom}}^{n-1} c_{\rm dev}(l) \tag{11}$$

where $\hat{L}_{\rm nom}$ is the nominal delay $L_{\rm nom}$ rounded to the nearest integer. The summation is thus performed over the delay corresponding to the distance between the two observation points. Note that, as in (8), the sum in (11) is over time, i.e., the delay line corresponds to the delay it takes a wave to travel from x_1 to x_2 and that this delay is not constant. However, since the deviation in delay is small, it is convenient to compute the sum over a constant delay of integer-valued length. Note that we assume that $c_{\rm dev}(n)$ is defined on the range $[-\hat{L}_{\rm nom}(n) - 1,\,\infty)$. It is convenient to define $c_{\rm dev}(n) = 0, \qquad n < 0$.

The summation in (11) may be implemented computationally efficiently with a delay line of $\hat{L}_{\rm nom}$ unit delays and a state variable that stores the current value $d(n)$. During each sampling interval we only need to subtract the value exiting the delay line from $d(n)$ and add the value entering the delay line. The transfer function for the boxcar summation is $I_{\rm box}(z) = (1 - z^{-\hat{L}_{\rm nom}})/(1 - z^{-1})$.

We may also approximate the boxcar summation of (11) using a leaky integrator with a transfer function

$$I(z) = g_p\frac{1 + a_p}{1 + a_p z^{-1}} \tag{12}$$

where $-1 < a_p < 0$ and g_p is a gain term. The parameters of the leaky integrator of (12) may be matched to the boxcar integration, e.g., by requiring that the sums of the impulse responses of the two integrators match, and that the time constant of the leaky integrator equals the length of the boxcar summation. The time constant is defined to be the time in which the impulse response of the filter in (12) decays into $1/e$ of its maximum value (first sample) and it is computed as [24]

$$\tau = \frac{-1}{\ln(-a_p)}. \tag{13}$$

After the parameter a_p is computed using (13), it is straightforward to show that the parameter $g_p = \hat{L}_{\rm nom}$ if we require that $\sum_{k=0}^{\infty} i(n) = \sum_{k=0}^{\infty} i_{\rm box}(n)$, where $i(n)$ and $i_{\rm box}(n)$ are the impulse responses of the leaky integrator of (12) and of the boxcar integrator, respectively. In sound synthesis applications, the parameters of the leaky integrator may be used to control the pitch variation and the coupling of the harmonics separately as demonstrated in Section IV.

The finite-length digital waveguide with uniformly time-varying propagation speed may be identified as a special case of a general nonlinear delay line with a signal-dependent time-varying fractional delay (TVFD) filter parameter [9]. The TVFD structure is illustrated in Fig. 4. The function G maps the signal in the delay line into a delay parameter $d(n)$ that controls the fractional delay filter.

IV. Discrete-Time Simulation of Vibrating String Tension Modulation

With the developments of the previous section, we may now proceed to a bidirectional digital waveguide model that simulates a string with tension modulation. Such a model is depicted in Fig. 5. The upper and lower delay lines together with the elongation approximation and computation of the delay parameter $d(n)$ may be identified as two TVFD structures presented in Fig. 4. The transfer functions $R_f(z)$ and $R_b(z)$ model the wave reflections at the fret and at the bridge, respectively. The output of the model is taken at the bridge, corresponding to the case of, e.g., the acoustic guitar [13]. For the model to be complete we need to define the two blocks of elongation approximation and delay-parameter $d(n)$ computation.

A. Elongation Approximation

The elongation of a string is given by (1) where it is observed that it essentially depends on the first spatial derivative of the displacement, i.e., the slope. It is thus natural to choose slope as the wave variable for the digital waveguide. When slope waves are used, the reflection filters $R_f(z)$ and $R_b(z)$ are inverting, as would be the case with, e.g., velocity waves. Note that while in the linear case the conversion between wave variables is straightforward, in the nonlinear case it is not directly possible in general. The elongation of the string may be approximated by developing (1) for the digital waveguide as

$$L_{\rm dev}(n) = \sum_{k=0}^{\hat{L}_{\rm nom}-1} \sqrt{1+[s_r(n,\,k)+s_l(n,\,k)]^2} - \hat{L}_{\rm nom} \tag{14}$$

where $s_r(n,\,k)$ and $s_l(n,\,k)$ are, respectively, the right and left going slope waves at position k and time instant n. The slope waves thus correspond to the first spatial derivative of the displacement in samples. The use of the rounded nominal string length $\hat{L}_{\rm nom}$ in (14) is typically sufficiently accurate since the discrepancy is always limited to 1/2 samples which is small compared to $L_{\rm nom}$ with practical sampling frequencies.[1]

[1]For instance, at a sampling frequency of 44 100 Hz, the E[5] tone of 659 Hz corresponds to $L_{\rm nom} = 33.46$ samples, $\hat{L}_{\rm nom} = 33$ samples, and the discrepancy is 0.46 samples, i.e., 1.4%.

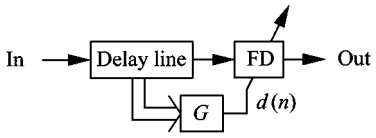

Fig. 4. General nonlinear delay line that is implemented with the TVFD structure [9]. The function G maps the contents of the delay line onto the delay variable $d(n)$ that controls the fractional delay filter.

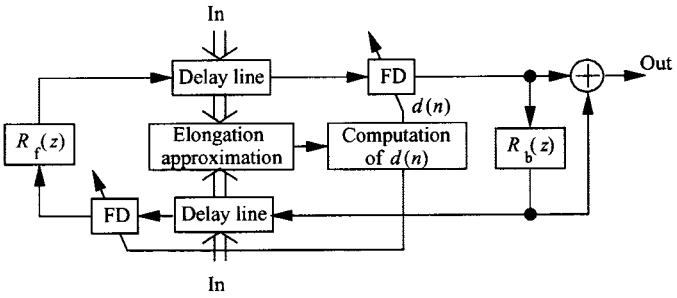

Fig. 5. Dual-delay line model implementing the tension modulation with signal-dependent fractional delay elements.

While the elongation given by (14) is readily applicable for a simulation, it may be advantageous in practical implementations to approximate it with a computationally more efficient formula. If we assume that $[s_r(n,\,k)+s_l(n,\,k)]^2 \ll 1$, we may develop a truncated Taylor series approximation of (14). Note that the assumption made when developing the linear wave equation is $|\partial y/\partial x| \ll 1$ which corresponds to $|[s_r(n,\,k)+s_l(n,\,k)]| \ll 1$ in the discrete-time formulation. Now we only assume that $(\partial y/\partial x)^2 \ll 1$. With the truncated Taylor series approximation we obtain

$$\begin{aligned} L_{\rm dev}(n) &\approx \sum_{k=0}^{\hat{L}_{\rm nom}-1} \left[1+\tfrac{1}{2}[s_r(n,\,k)+s_l(n,\,k)]^2\right] - \hat{L}_{\rm nom} \\ &= \tfrac{1}{2} \sum_{k=0}^{\hat{L}_{\rm nom}-1} [s_r(n,\,k)+s_l(n,\,k)]^2. \end{aligned} \tag{15}$$

The use of the truncated Taylor series approximation reduces the computational complexity of the elongation approximation since the square-root operation is removed. In Section IV-B, we describe how the approximated elongation is used to compute the time-varying delay parameter $d(n)$ of Fig. 5.

B. Computation of the Delay Parameter

The deviation of time-varying propagation speed of (3) from the nominal speed $c_{\rm nom}$ may be written for the discrete-time case as

$$c_{\rm dev}(n) = c_{\rm nom}\sqrt{1+(1+A)\frac{L_{\rm dev}(n)}{L_{\rm nom}}+A\left(\frac{L_{\rm dev}(n)}{L_{\rm nom}}\right)^2} - c_{\rm nom} \tag{16}$$

where $A = ES/F_{\rm nom}$. The time-varying delay parameter is obtained using (11) and (16) as

$$\begin{aligned} d(n) &= -T \sum_{l=n-1-\hat{L}_{\rm nom}}^{n-1} \\ &\quad \cdot \left[c_{\rm nom} \sqrt{1+(1+A)\frac{L_{\rm dev}(l)}{L_{\rm nom}} + A\left(\frac{L_{\rm dev}(l)}{L_{\rm nom}}\right)^2} \right. \\ &\quad \left. - c_{\rm nom} \right] \\ &= - \sum_{l=n-1-\hat{L}_{\rm nom}}^{n-1} \\ &\quad \cdot \left[\sqrt{1+(1+A)\frac{L_{\rm dev}(l)}{L_{\rm nom}} + A\left(\frac{L_{\rm dev}(l)}{L_{\rm nom}}\right)^2} - 1 \right] \end{aligned} \tag{17}$$

where $Tc_{\rm nom} = 1$ since T is the sampling interval and $c_{\rm nom}$ equals the sampling frequency, and $L_{\rm dev}(l)$ is given by either (14) or (15), depending on the desired accuracy and computational capacity.

In order to simplify (17) for a computationally more efficient implementation, it is useful to examine the range of values the parameter $A = ES/F_{\rm nom}$ may have. For a typical high-E string of an acoustic guitar with nylon strings $E = 5 \times 10^8$ N/m^2, $S = 3.6 \times 10^{-7}$ m^2, and $F_{\rm nom} = 82$ N [25], yielding $A = 180$. For a steel string the nominal string tension may be 50% greater than that of the nylon string, and Young's modulus is approximately 40 times that of the nylon string [25]. However, the string diameter may be ten times smaller than that of the nylon string, and thus the value of A is only several times larger than that of the nylon string. The length of the string in a typical acoustic guitar is approximately 0.65 m, and the maximum displacement may be several millimeters. For a displacement of 2.0 mm at the middle of the string, the relative elongation is

$$\frac{\ell_{\rm dev}}{\ell_{\rm nom}} = 2\frac{\sqrt{0.325^2 + 0.0020^2} - 0.325}{0.325} = 3.8 \times 10^{-5}.$$

Thus the second-order term $A(L_{\rm dev}(n)/L_{\rm nom})^2$ is typically negligible. If computational efficiency is emphasized, the square root in (17) may be approximated by the first terms of a Taylor series, assuming $(1+A)(L_{\rm dev}(n)/L_{\rm nom}) \ll 1$, as

$$d(n) \approx -\frac{1}{2} \sum_{l=n-1-\hat{L}_{\rm nom}}^{n-1} (1+A)\frac{L_{\rm dev}(l)}{L_{\rm nom}}. \tag{18}$$

The output signal of the model may be a force signal at the bridge of an acoustic guitar or a pickup voltage in an electric guitar. In the first case the output signal is related to the difference of the velocity waves at the bridge [4], and in the latter case to the velocity output signal, i.e., the sum of the two velocity waves. Thus, a conversion from slope waves $s(n,\, k)$ to velocity waves $v(n,\, k)$ is required. In the linear case the two waves are related through the time-invariant propagation speed $c_{\rm nom}$ as $v_l(n,\, k) = c_{\rm nom} s_l(n,\, k)$ and $v_r(n,\, k) = -c_{\rm nom} s_r(n,\, k)$ [4]. The velocity wave can thus be computed by subtracting the left-going wave from the right-going wave and multiplying by the propagation speed. In the nonlinear case the conversion is not so straightforward. However, it still seems reasonable to approximate the output velocity signal at position k as $v(n) = v_r(n,\, k) + v_l(n,\, k) = c_{\rm nom}(s_l(n,\, k) - s_r(n,\, k))$, since the deviation term $c_{\rm dev}(n)$ is small compared to the nominal propagation speed $c_{\rm nom}$.

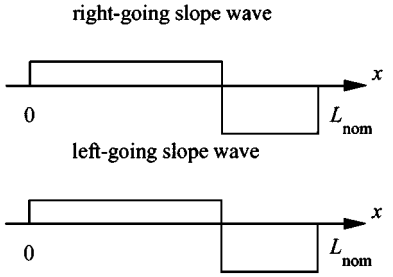

Fig. 6. Initial slope wave variables for the dual-delay-line model corresponding to an ideal pluck at a distance of $1/3L_{\rm nom}$ from the string termination.

In the linear case, the input signal can be fed at a single point of the digital waveguide if acceleration waves are used [26], [27]. With the nonlinear model using slope variables, the input signal is a distribution that is inserted in the two delay lines. Similarly, if the virtual string is plucked while it still vibrates, the input signal has to be gradually added at all the positions of the delay lines. Fig. 6 illustrates the initial slope variable distribution along the two delay lines corresponding to an ideal pluck[2] at a distance of $1/3L_{\rm nom}$ from the termination. The slope variables are piecewise constant and identical in the two delay lines. It is possible to feed the input signal only to a single position of the delay line. However, this results in inaccuracy of the elongation estimation at the beginning of the signal.

Methods to obtain the parameter A from recorded plucked-string tones are described in Section V. Synthesis examples of the model of Fig. 5 are described in Section VI. In the following, we reduce the dual-delay-line model into a computationally more efficient single-delay-loop model.

C. Single-Delay-Loop Model with Tension Modulation

In the linear case it is straightforward to reduce the dual-delay-line model of Fig. 5 into a single-delay-loop (SDL) model that includes a loop with a delay line, fractional delay filter, and a loop filter that consolidates the reflection filters $R_b(z)$ and $R_f(z)$, and a comb-filter for the pluck-position effect [13]. It is obvious that the SDL model is computationally more efficient than the dual-delay-line model. While commutation is not allowed in general in nonlinear models, we present an SDL model with tension modulation nonlinearity that approximates the model of Fig. 5. Examples of synthetic tones obtained with the dual-delay-line and the single-delay-loop models are available through the Internet [21].

[2]By ideal pluck we refer to initial conditions in which the string is released with no initial velocity and a displacement distribution in the shape of a triangle.

Combining the two delay lines requires the commuting of one of the reflection filters and a delay line. Thereafter the filters can be consolidated. In this case the commutation changes the contents of the delay lines little since the magnitude of the reflection filters is very close to unity [13]. Fig. 7 shows this intermediate stage in developing the single-delay-line model. Loop filter $H_l(z)$ now represents the composite lowpass filtering effect of $R_b(z)$ and $R_f(z)$. Notice also how the output of the model is simplified. The output transfer function $1 + R_b(z)$ in Fig. 5 may be replaced with a constant multiplier with negligible effect in the output signal since the frequency response $R_b(e^{j\omega})$ is very close to 1 at all frequencies, as explained in [13].

The two time-varying FD filters may also be combined into a single TVFD unit. This FD element is placed at the end of the delay lines which may then be combined into a single delay line that is twice as long as each of the delay lines in Fig. 5. The resulting single-delay-loop string model is presented in Fig. 8. The elongation estimation in Fig. 8 is equivalent to that shown in the dual-delay-line model (Fig. 5) and it consists of summing the first sample of the delay line with the last one, the second sample with the second last one, and so on, squaring all the sums, and summing them up according to (15).

The delay line initialization should account for the fact that the reflection filter and the delay line are commuted. Since slope waves are used, the initial contents of the delay lines in Fig. 6 may be directly aggregated. An example of initial contents of the single-delay-line model corresponding to an ideal pluck at a distance of $1/3L_{\rm nom}$ is depicted in Fig. 9. Note that if, e.g., velocity waves were used, the reflection filters would be inverting and that would have to be taken into account by inverting the left-going (or right-going) wave before aggregation.

D. Reduced-Complexity Estimation of Elongation

The string-length estimation is the most time-consuming operation in both the dual-delay-line model of Fig. 5 and the single-delay-loop model of Fig. 8. The computational burden of the string-length estimation depends on the nominal string length $L_{\rm nom}$ as can be seen in (14) and (15), and with low tones it requires hundreds of addition and multiplication operations per sampling interval. The computational cost of the other string model components is independent of $L_{\rm nom}$ and they typically require only 10–20 operations.

A simple way to reduce the computational burden of the squared sum is to approximate it with a *sparse squared sum*, where every Mth sample pair is included but the rest of the pairs are excluded. The sparse squared sum must be scaled by M to compensate the total magnitude. For instance, for a 147 Hz tone at a sampling frequency of 22 050 Hz, the nominal string length is 75 samples. Using (15) we have to complete 149 additions and 76 multiplications for approximation of the elongation. Using the sparse-squared-sum approximation with $M = 6$, we have 12 summing points yielding 23 additions and 13 multiplications. The sparse-squared-sum approximation may be considered a spatial downsampling and it is justified by the fact that summing over the string produces a lowpass-filtering effect on the tension modulation. Examples in Section VI illustrate the results of this method.

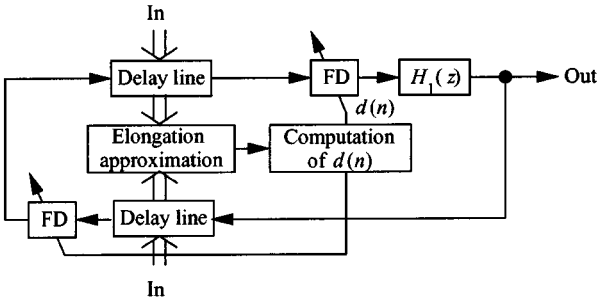

Fig. 7. Dual-delay line model where the reflection filters have been commuted and combined. The output of the model is also simplified.

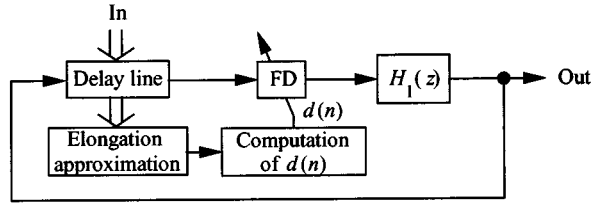

Fig. 8. Single-delay-loop model for simulation of a vibrating string with tension modulation.

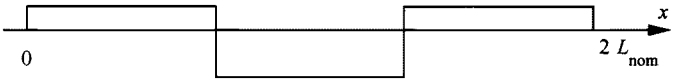

Fig. 9. Initial slope wave variables for the single-delay-line model of Fig. 8 corresponding to an ideal pluck at a distance of $1/3L_{\rm nom}$ from the string termination.

V. Parameter Estimation

If a linear model is used for synthesis, the model parameters may be analyzed using a methodology described in [28]–[30]. The parameter estimation may be divided into three subproblems, namely, estimation of the fundamental frequency, design of a loop filter that optimally reproduces the frequency-dependent decay of vibration of the autonomously vibrating string, and computation of an excitation signal. When the tension modulation nonlinearity is added, an additional task is to estimate the modulation depth in the original signal. In this study, we have used isolated tones of acoustic and electric guitars recorded in an anechoic chamber for parameter estimation. We apply the previously reported methods that were developed to parameter estimation in the linear case [28], [29] and develop a technique for estimation of the tension modulation parameters.

A. Estimation of Parameters for the Linear String Model

The nominal fundamental frequency $f_{0,\,\rm nom}$ may be obtained from the short-time autocorrelation function that is computed on the tail of the tone where the tension modulation effect is small. The estimated nominal string length is given by the nominal fundamental frequency as $L_{\rm nom} = f_s/2f_{0,\,\rm nom}$ where f_s is the sampling frequency.

The loop-filter parameters are obtained using techniques presented in [28]–[30] that apply sinusoidal modeling [31], [32]. The amplitude envelopes of the decaying partials are detected in a short-time Fourier transform of the recorded signal and the loop filter is optimized to yield similar decay-time-constants for

the partials of the synthetic signal. A one-pole loop filter is used in this study since it has been found a good compromise between computational efficiency and simulation accuracy [28], [29]. Estimation of the loop-filter parameters is detailed in [28], [29]; another approach using heterodyne filtering is described in [30].

In the linear case, the excitation signal may be obtained by canceling the decaying partials in the recorded tone by inverse filtering [28] or by subtraction of the sinusoidal model and equalizing the attack part of the residual signal [29], [30]. The synthesis technique using this kind of excitation signal is called commuted waveguide synthesis (CWS) [33], [34] referring to the commuting of the body response with the string model. In the nonlinear case the CWS technique is not applicable, and we may not aggregate the pluck with the body response. The body response may be simulated with a linear filter that models the impulse response of the body driven at the bridge. In this case it is advantageous to separate the most prominent body responses and resynthesize them with, e.g., parametric second-order resonators that are in cascade with the digital filter modeling the rest of the body response [35], [29], [30]. Note that we are no longer able to obtain an exact replica of the recorded tone since the inverse-filtering technique used in CWS is not applicable. However, the proposed method together with the parameter estimation methods allow for better control of the instrument behavior, in particular, the tension modulation nonlinearity.

Models have recently been presented for plucking a string with finger [36]–[38]. In this study we assume an ideally plucked string and discard the dynamics of the plucking event. Thus, the initial slope distributions in the two waveguides are defined by the maximum displacement and the plucking position.

B. Estimation of Parameters for the Tension Modulation Model

Inspection of (17) reveals that the variation of the delay parameter $d(n)$ depends on the parameter A and the string length deviation $L_{\rm dev}(n)$. Since we are only able to observe the nonlinearity from a recorded tone via the varying fundamental frequency and generation of missing harmonics, estimation of these parameters directly is difficult. Rather, we match A and $L_{\rm dev}(n)$ to produce the desired pitch variation. Parameter A can also be derived from the Young's modulus E, the cross sectional area S, and the nominal tension $F_{\rm nom}$ of the string if such data are available. In some cases the maximum displacement of the string is estimated during the recording, and estimation of A by analysis of the recorded tone is straightforward, as described below.

If no information about the maximum displacement is available, a suitable value may be chosen according to the recorded tone. We compute the average of the elongation $\langle L_{\rm dev}\rangle$ over the first period of string vibration using the nominal propagation speed $c_{\rm nom}$. From the estimated time history of the fundamental frequency we obtain the maximum average delay parameter (corresponding to the maximum fundamental frequency) as

$$\langle d_{\max}\rangle = \frac{1}{2}\left(\frac{f_s}{f_{0,\max}} - \frac{f_s}{f_{0,\rm nom}}\right) \tag{19}$$

where $f_{0,\max}$ is the maximum value of the detected fundamental frequency. In (19) the difference is divided by 2 since the varying delay is implemented with two fractional delay filters when the dual-delay-line model of Fig. 5 is used. For the single-delay-loop model, the varying delay is $2\langle d_{\max}\rangle$.

By substituting $\langle d_{\max}\rangle$ for $d(n)$ and $\langle L_{\rm dev}\rangle$ for $L_{\rm dev}(n)$ in (17), we obtain

$$\langle d_{\max}\rangle = -L_{\rm nom}\sqrt{1+(1+A)\frac{\langle L_{\rm dev}\rangle}{L_{\rm nom}}+A\left(\frac{\langle L_{\rm dev}\rangle}{L_{\rm nom}}\right)^2} + L_{\rm nom}. \tag{20}$$

Parameter A may be solved from (20) as

$$\begin{aligned}
&\sqrt{1+(1+A)\frac{\langle L_{\rm dev}\rangle}{L_{\rm nom}}+A\left(\frac{\langle L_{\rm dev}\rangle}{L_{\rm nom}}\right)^2} \\
&\quad = 1-\frac{\langle d_{\max}\rangle}{L_{\rm nom}} \\
&A\left(\frac{\langle L_{\rm dev}\rangle}{L_{\rm nom}}+\frac{\langle L_{\rm dev}\rangle^2}{L_{\rm nom}^2}\right) \\
&\quad = \left(1-\frac{\langle d_{\max}\rangle}{L_{\rm nom}}\right)^2 - \frac{\langle L_{\rm dev}\rangle}{L_{\rm nom}} - 1 \\
&A = \frac{\left(1-\frac{\langle d_{\max}\rangle}{L_{\rm nom}}\right)^2 - \frac{\langle L_{\rm dev}\rangle}{L_{\rm nom}} - 1}{\frac{\langle L_{\rm dev}\rangle}{L_{\rm nom}}+\frac{\langle L_{\rm dev}\rangle^2}{L_{\rm nom}^2}}.
\end{aligned} \tag{21}$$

Similarly, we may estimate the maximum average elongation $\langle L_{\rm dev}\rangle$ using (21) if A is known.

An example of the determination of the parameter A follows. The maximum fundamental frequency of the acoustic guitar tone in bottom of Fig. 2 is approximately $f_{0,\max} = 150.4$ Hz and the nominal fundamental frequency is $f_{0,\rm nom} = 149.8$ Hz; thus, from (19) $\langle d_{\max}\rangle = -0.39$ with a sampling frequency of 22 050 Hz. The nominal string length corresponds approximately to $L_{\rm nom} = 75$ samples. If we assume that the maximum displacement of the string with a length of 0.65 m is 0.001 m, $A = 3500$. If we assume that the displacement is 0.002 m, $A = 870$. Note that our method of detecting parameter A is not a reliable method to derive information about the string properties from the recorded tone. It is only used to derive the tension modulation depth for given displacement so that the original pitch variation is reproduced in the synthetic tone.

With the parameter estimation method described above we are able to produce synthetic tones that have similar tension modulation effects to the original tone. In Section VI we demonstrate the performance of the model with analysis/synthesis examples.

VI. Analysis/Synthesis Experiments

In this context, we discuss synthetic tones that were obtained using

1) linear model;
2) nonlinear dual-delay line model of Fig. 5;
3) nonlinear SDL model of Fig. 8;

4) nonlinear sparse-squared-sum SDL model.

These signals together with more audio examples are available through the WWW [21].

The signals have a nominal fundamental frequency of 147 Hz, the A parameter is 766, and the initial displacement is assumed 2.0 or 4.0 mm on a string with length of 0.65 m. The displacement of 2.0 mm corresponds to the initial displacement used to estimate the parameter A from the recorded tone in Section V. The leaky integrator of (12) is used in the SDL models. We have used a sampling frequency of 22 050 Hz in the simulations and the nominal string length $L_{\rm nom} = 75$ samples. The loop-filter parameters were estimated using the method based on sinusoidal modeling, and they were $a_1 = -0.0014$ and $g = 0.9880$. The plucking position was 1/3 of the string length from the bridge. The sparse-squared-sum parameter is $M = 6$. In the pitch variation examples of Section VI-A, the a_p parameter of the leaky integrator used in the SDL models is obtained using (13) and it is -0.9868. As described in Section III-B, the value of g_p parameter is 75.0. In the examples of Section VI-B, these parameters are varied. Note that it is practical to combine the term $g_p(1+a_p)$ from (12) with the term $-(1+A)/2L_{\rm nom}$ from (18) into a single multiplying coefficient when implementing the SDL model with tension modulation nonlinearity.

A. Pitch Variation

Figs. 10 and 11 depict the estimated fundamental frequency trajectories of the synthetic tones obtained using the nonlinear dual-delay-line model (solid line), the nonlinear SDL model (dashed line), and the nonlinear sparse-squared-sum SDL model (dash-dot line). In Fig. 10 the pitch variation has been designed to match the 0.6 Hz deviation detected in the steel-stringed acoustic guitar tone of Fig. 2. In Fig. 11 we choose the initial displacement larger than when estimating the value of the parameter A. Thus, we expected the pitch variation to be larger than in the original recorded guitar tone on the bottom Fig. 2. This is indeed the case since all the synthetic models exhibit a pitch variation of approximately 2.5 Hz. This suggests that our model behaves physically correctly since the pitch variation is increased by increasing the initial displacement. Comparing the results of Fig. 10 to the pitch deviation in the original tone shown in the bottom plot of Fig. 2, it is seen that the amplitude and decay of deviation of the fundamental frequency are relatively well matched to the original tone. The nominal fundamental frequencies of the tones are not the same since the fundamental frequency trajectory of the recorded tone approaches 146 Hz while that of the synthetic tone approaches 147 Hz. This is easily corrected by adjusting the nominal string length in the synthetic tone. In Figs. 10 and 11 the curves obtained with different implementations of the model behave similarly.

B. Coupling of Harmonics

As discussed by Legge and Fletcher, the tension modulation nonlinearity together with nonrigid end support provides means for coupling of the harmonic modes [19]. Since we have not incorporated a detailed model of the bridge in this simulation and we assume that there is only slight frequency-dependent damping at the terminations, we expect the coupling between the harmonic modes to be small. Note that in actual instruments the terminations are nonrigid and the harmonic mode coupling is more pronounced.

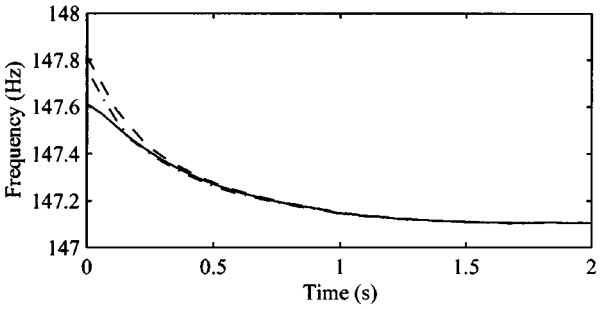

Fig. 10. Time-varying fundamental frequency as detected from synthesized tones obtained using the nonlinear dual-delay-line model (solid line), the nonlinear single-delay-loop model (dashed line), and the nonlinear single-delay-loop model with the sparse-squared-sum ($M = 6$) computation (dash-dot line). The fundamental frequency variation is designed to be 0.6 Hz. The initial slope distributions correspond to an initial displacement of 2 mm on a string with a length of 0.65 m. The plucking position is one third of a string length from the termination.

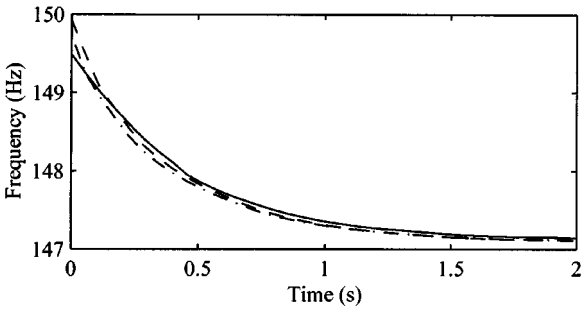

Fig. 11. Time-varying fundamental frequency as detected from synthesized tones obtained using the nonlinear dual-delay-line model (solid line), the nonlinear single-delay-loop model (dashed line), and the nonlinear single-delay-loop model with the sparse-squared-sum computation (dash-dot line). The initial slope distributions correspond to an initial displacement of 4 mm on a string with a length of 0.65 m. The plucking position is one third of a string length from the termination.

The coupling of harmonic modes is most clearly detectable by the phenomenon of generation of missing harmonics. If a linear string is plucked at a position that is exactly at a node of a harmonic mode, that mode will not be excited. In the nonlinear string where the harmonic modes are coupled, such a harmonic will in general start to vibrate since it is effectively driven by other harmonic modes. In the simulation, we plucked the virtual string at a distance of one third string length from the bridge, and thus in the linear case every third harmonic is missing. Fig. 12(a) illustrates the magnitude spectrum of a tone obtained using the linear dual-delay line model, and Fig. 12(b) the spectrum of a tone obtained with the nonlinear dual-delay line model. As expected, in the linear case the harmonics are completely missing and in the nonlinear case the spatially almost orthogonal harmonic modes prohibit any significant coupling; the magnitudes of every third harmonic are considerably smaller than those of the other harmonic modes.

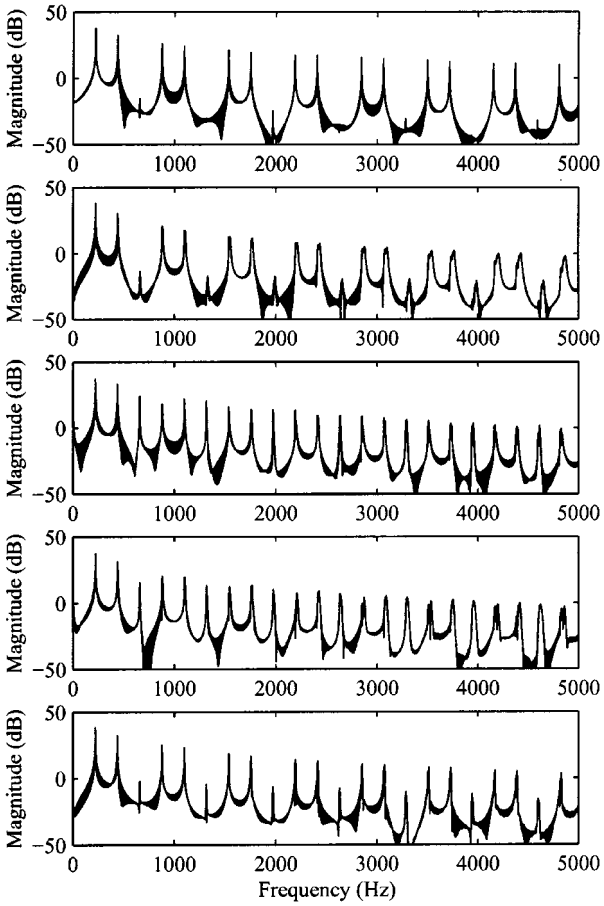

Fig. 12. Generation of missing harmonics. Magnitude spectra of synthetic tones obtained with (a) the linear dual-delay-line model, (b) the nonlinear dual-delay-line model using boxcar integration, (c) the SDL model using the leaky integrator with $a_p = -0.97$, (d) the SDL model with $a_p = -0.995$, and (e) the SDL model with $a_p = -0.999$.

For sound synthesis purposes, it may be attractive to use a model that permits the harmonic mode coupling. It turns out that if the boxcar integrator is replaced with the leaky integrator of (12), the harmonic modes become coupled. Furthermore, the extent of coupling may be controlled with the parameters of the leaky integrator. Fig. 12(c)–(e) illustrate the harmonic mode coupling when the nonlinear SDL model is used with the leaky integrator. The leaky integrator parameter a_p is -0.97, -0.995, and -0.999 in the three plots, respectively, and the parameter $g_p = 75.0$. It is seen that with $a_p = -0.97$, when the effective integration length is considerably shorter than in the boxcar integration in this case, the magnitudes of the initially missing harmonic modes are comparable to those of the neighboring harmonics. Increasing the effective length of integration by increasing the value of a_p reduces the harmonic mode coupling effect, as illustrated in Fig. 12(d) and (e).

Note that modification of the leaky integrator parameters results in synthetic tones that are not authentic in the sense that the tension modulation simulation with altered integration parameters does not correspond to the physical behavior of the string. However, from a sound synthesis and perceptual viewpoint, the pitch variation and coupling of harmonic modes may be parametrically and intuitively controlled to obtain synthetic tones that retain the string character.

VII. Conclusions

In this paper, a nonlinear model was developed for the simulation of a string exhibiting tension modulation nonlinearity. It was shown that the tension-modulated string may be simulated with a digital waveguide model with uniformly distributed time-varying propagation velocity that is controlled by the elongation of the string. The structure was first formulated with two time-varying fractional delay filters and it was then simplified into a single-delay-loop model with only one TVFD filter. The computational complexity was further reduced by simplifying the elongation computation using a sparse-squared-sum structure. A technique was described for estimation of the modulation depth parameter from recorded plucked-string instrument tones. The validity and performance of the model was demonstrated by analysis/synthesis examples and synthetic tones available via the WWW [21].

While the proposed model is not capable of exact resynthesis, the synthesized tones demonstrate that it essentially captures the two perceptually most important tension modulation effects, namely, variation of the fundamental frequency and coupling of the harmonic components. With the nonlinear effects, the synthesized tones appear more lively mainly due to subtle variations in the timbre of the tones similar to real plucked-string tones.

References

[1] V. Välimäki, T. Tolonen, and M. Karjalainen, "Plucked-string synthesis algorithms with tension modulation nonlinearity," in *Proc. IEEE ICASSP*, vol. 2, Phoenix, AZ, Mar. 1999, pp. 977–980.

[2] *Information technology—Coding of audiovisual objects—Part 3: Audio*, ISO/IEC FCD Std. 14 496-3, 1998.

[3] J. O. Smith, "Music applications of digital waveguides," Dept. Music, Stanford University, Stanford, CA, Tech. Rep. STAN-M-39, CCRMA, May 1987.

[4] ——, "Physical modeling using digital waveguides," *Comput. Music J.*, vol. 16, no. 4, pp. 74–91, 1992.

[5] ——, "Physical modeling synthesis update," *Comput. Music J.*, vol. 20, no. 2, pp. 44–56, 1996.

[6] R. Msallam, S. Dequidt, S. Tassart, and R. Caussè, "Physical model of the trombone including nonlinear propagation effects," in *Proc. Inst. Acoustics*, vol. 19, Edinburgh, U.K., Sept. 1997, pp. 245–250.

[7] S. Tassart, R. Msallam, P. Depalle, and S. Dequidt, "A fractional delay application: Time-varying propagation speed in waveguides," in *Proc. Int. Computer Music Conf.*, Thessaloniki, Greece, Sept. 1997, pp. 256–259.

[8] J. R. Pierce and S. A. Van Duyne, "A passive nonlinear digital filter design which facilitates physics-based sound synthesis of highly nonlinear musical instruments," *J. Acoust. Soc. Amer.*, vol. 101, pp. 1120–1126, Feb. 1997.

[9] V. Välimäki, T. Tolonen, and M. Karjalainen, "Signal-dependent nonlinearities for physical models using time-varying fractional delay filters," in *Proc. Int. Computer Music Conf.*, Ann Arbor, MI, Oct. 1998, pp. 264–267.

[10] E. Rank and G. Kubin, "A waveguide model for slapbass synthesis," in *Proc. IEEE ICASSP*, vol. 1, Munich, Germany, Apr. 1997, pp. 443–446.

[11] J. O. Smith, "Nonlinear commuted synthesis of bowed strings," in *Proc. Int. Computer Music Conf.*, Thessaloniki, Greece, Sept. 1997, pp. 264–267.

[12] M. Karjalainen, J. Backman, and J. Pölkki, "Analysis, modeling and real-time synthesis of the kantele, a traditional Finnish string instrument," in *Proc. IEEE ICASSP*, vol. 1, Minneapolis, MN, Apr. 1993, pp. 229–232.

[13] M. Karjalainen, V. Välimäki, and T. Tolonen, "Plucked string models: From Karplus–Strong algorithm to digital waveguides and beyond," *Comput. Music J.*, vol. 22, no. 3, pp. 17–32, 1998.

[14] G. F. Carrier, "On the nonlinear vibration problem of the elastic string," *Q. Appl. Math.*, vol. 3, pp. 157–165, 1945.

[15] R. Narasimha, "Non-linear vibration of an elastic string," *J. Sound Vib.*, vol. 8, no. 1, pp. 134–146, 1968.

[16] W. C. Elmore and M. A. Heald, *Physics of Waves*, New York: Dover, 1969.
[17] G. V. Anand, "Large-amplitude damped free vibration of a stretched string," *J. Acoust. Soc. Amer.*, vol. 45, no. 5, pp. 1089–1096, 1969.
[18] P. M. Morse and U. K. Ingard, *Theoretical Acoustics*. Princeton, NJ: Princeton Univ. Press, 1968.
[19] K. A. Legge and N. H. Fletcher, "Nonlinear generation of missing modes on a vibrating string," *J. Acoust. Soc. Amer.*, vol. 76, pp. 5–12, July 1984.
[20] R. J. Hanson, J. M. Anderson, and H. K. Macomber, "Measurements of nonlinear effects in a driven vibrating wire," *J. Acoust. Soc. Amer.*, vol. 96, pp. 1549–1556, Sept. 1994.
[21] T. Tolonen, V. Välimäki, and M. Karjalainen. (1999) Sound examples for modeling of tension modulation nonlinearity in plucked strings. [Online]http://www.acoustics.hut.fi/~ttolonen/tmstr_SAP/.
[22] V. Välimäki, "Discrete-time modeling of acoustic tubes using fractional delay filters," Ph.D. dissertation, Helsinki Univ. Technol., Espoo, Finland, 1995.
[23] T. I. Laakso, V. Välimäki, M. Karjalainen, and U. K. Laine, "Splitting the unit delay—Tools for fractional delay filter design," *IEEE Signal Processing Mag.*, vol. 13, pp. 30–60, Jan. 1996.
[24] S. J. Orfanidis, *Introduction to Signal Processing*. Englewood Cliffs, NJ: Prentice-Hall, 1996.
[25] N. H. Fletcher and T. D. Rossing, *The Physics of Musical Instruments*, New York: Springer-Verlag, 1991.
[26] J. O. Smith, "Techniques for digital filter design and system identification with application to the violin," Ph.D. dissertation, Stanford Univ., Stanford, CA, June 1983.
[27] M. Karjalainen and U. K. Laine, "A model for real-time sound synthesis of guitar on a floating-point signal processor," in *Proc. IEEE ICASSP*, vol. 5, Toronto, Ont., Canada, 1991, pp. 3653–3656.
[28] V. Välimäki, J. Huopaniemi, M. Karjalainen, and Z. Jánosy, "Physical modeling of plucked string instruments with application to real-time sound synthesis," *J. Audio Eng. Soc.*, vol. 44, pp. 331–353, May 1996.
[29] T. Tolonen, "Model-based analysis and resynthesis of acoustic guitar tones," M.Sc. thesis, Helsinki Univ. Technol., Espoo, Finland, Jan. 1998.
[30] V. Välimäki and T. Tolonen, "Development and calibration of a guitar synthesizer," *J. Audio Eng. Soc.*, vol. 46, pp. 766–778, Sept. 1998.
[31] R. J. McAulay and T. F. Quatieri, "Speech analysis/synthesis based on a sinusoidal representation," *IEEE Trans. Acoust.. Speech, Signal Process.*, vol. 34, pp. 744–754, Aug. 1986.
[32] X. Serra, "A system for sound analysis/transformation/synthesis based on a deterministic plus stochastic decomposition," Ph.D. dissertation, Stanford Univ., Stanford, CA, 1989.
[33] J. O. Smith, "Efficient synthesis of stringed musical instruments," in *Proc. Int. Computer Music Conf.*, Tokyo, Japan, Sept. 1993, pp. 64–71.
[34] M. Karjalainen, V. Välimäki, and Z. Jánosy, "Toward high-quality sound synthesis of the guitar and string instruments," in *Proc. Int. Computer Music Conf.*, Tokyo, Japan, Sept. 1993, pp. 56–63.
[35] M. Karjalainen and J. O. Smith, "Body modeling techniques for string instrument synthesis," in *Proc. Int. Computer Music Conf.*, Hong Kong, Aug. 1996, pp. 232–239.
[36] M. Pavlidou and B. E. Richardson, "The string–finger interaction in the classical guitar," in *Proc. Int. Symp. Musical Acoustics*, Dourdan, France, July 1995, pp. 559–564.
[37] ——, "The string–finger interaction in the classical guitar: Theoretical model and experiments," in *Proc. Inst. Acoustics*, vol. 19, Edinburgh, U.K., Sept. 1997, pp. 55–60.
[38] G. Cuzzucoli and V. Lombardo, "Physical model of the plucking process in the classical guitar," in *Proc. Int. Computer Music Conf.*, Thessaloniki, Greece, Sept. 1997, pp. 172–179.

Tero Tolonen (S'98) was born in Oulu, Finland, in 1972. He majored in acoustics and audio signal processing and received the M.Sc.(Tech.) and Lic.Sc.(Tech.) degrees in electrical engineering from the Helsinki University of Technology (HUT), Espoo, Finland, in January 1998 and December 1999, respectively. He is currently pursuing a postgraduate degree.

He has been with the HUT Laboratory of Acoustics and Audio Signal Processing since 1996. His research interests include model-based audio representation and coding, physical modeling of musical instruments, and digital audio signal processing.

Mr. Tolonen is a student member of the IEEE Signal Processing Society and the Audio Engineering Society.

Vesa Välimäki (S'90–M'92–SM'99) was born in Kuorevesi, Finland, in 1968. He received the M.Sc.(Tech.), Lic.Sc.(Tech.), and Dr.Sc.(Tech.) degrees in electrical engineering from the Helsinki University of Technology (HUT), Espoo, Finland, in 1992, 1994, and 1995, respectively.

Since 1990, he has been with the Laboratory of Acoustics and Audio Signal Processing, HUT. In 1996, he spent six months as a Postdoctoral Research Fellow with the University of Westminster, London, U.K. He then returned to HUT, where he holds the position of Senior Assistant. Currently, he is on leave as a Postdoctoral Researcher at the Academy of Finland. In April 1999, he was appointed Docent in Audio Signal Processing at HUT. His research interests are in musical signal processing, active noise control, and digital filter design. He has published more than 70 journal articles and conference papers.

Dr. Välimäki is a senior member of the IEEE Signal Processing Society, the Audio Engineering Society, the International Computer Music Association, and the Acoustical Society of Finland. He is the Secretary of the IEEE Finland section.

Matti Karjalainen (M'84) was born in Hankasalmi, Finland, in 1946. He received the M.Sc. and the Dr.Tech. degrees in electrical engineering from the Tampere University of Technology, Tampere, Finland, in 1970 and 1978, respectively. His doctoral dissertation dealt with speech synthesis by rule in Finnish.

From 1980 to 1986, he was Associate Professor and since 1986, he has been a Full Professor of acoustics with the Faculty of Electrical Engineering, Helsinki University of Technology, Espoo, Finland. His research activities cover speech synthesis, analysis, and recognition, auditory modeling and spatial hearing, DSP hardware, software, and programming environments, as well as various branches of acoustics, including musical acoustics and modeling of musical instruments.

Dr. Karjalainen is a fellow of the AES and a member of ASA, EAA, ICMA, ESCA, and several Finnish scientific and engineering societies. He was the General Chair of the 1999 IEEE Workshop on Applications of Audio and Acoustics, New Paltz, NY.